JOURNAL OF SOLID STATE CHEMISTRY **1**, 583–592 (1970)

Thermodynamic Properties of Nickel-Tellurium Alloys

M. ETTENBERG†

RCA Laboratories, Princeton, New Jersey 08540

K. L. KOMAREK

Department of Inorganic Chemistry, University of Vienna, Vienna, Austria

AND

E. MILLER

Department of Mechanical Engineering, California State College at Long Beach, Long Beach, California 90021

Received September 2, 1969

Activities of tellurium in nickel-tellurium alloys were determined by an isopiestic method between 500° and 950°C and between 40 and 66 at % Te. From the activities partial molar quantities for the δ-NiAs–Cd(OH)$_2$ phase between 53 and 66.6 at % Te were calculated. Activities of tellurium exhibit a very pronounced concentration dependence near the tellurium- and nickel-rich phase boundaries with an inflection point at about 59 at % Te. The partial molar enthalpy $\Delta\bar{H}_{Te}$ was found to have a constant value of −14.8 kcal/g-atom between 53 and 60 at % Te followed by a decrease to −7.0 kcal/g-atom at 66.6 at % Te. Based on a statistical model of random distribution of nickel atoms over the 00 1/2 layers, activities and partial molar entropies were calculated which agreed well with the experimental values in the region of constant $\Delta\bar{H}_{Te}$. From the breaks in the temperature-composition curves phase boundaries were determined and the range of existence of the δ phase was established.

Nonstoichiometric compounds are one of the most important subjects of solid state chemistry. It has been known for a long time that in the Ni-Te system two ordered compounds, NiTe and NiTe$_2$, exist with a continuous range of solid solutions between them, thus forming one nonstoichiometric compound with a very wide range of homogeneity. Oftedal (*1*) found that NiTe has a hexagonal structure of the NiAs-(B8)-type. Tengnér (*2*) reported NiTe$_2$ to have the hexagonal Cd(OH)$_2$-(C6)-type structure. Klemm and Fratini (*3*) studied the region between NiTe and NiTe$_2$ by X-ray diffraction, density and magnetic susceptibility measurements and observed complete solubility at room temperature. Schneider and Imhagen (*4*) confirmed the range of homogeneity between NiTe and NiTe$_2$ by lattice parameter measurements between room temperature and 800 °C. The same results were obtained by Shchukarev and Apurina (*5*) for alloys between NiTe (50.0 at % Te) and NiTe$_{1.95}$ (66.2 at % Te) with a limiting composition of NiTe$_{\geq 1.7}$ (63.0 at % Te) at 900 °C. Westrum and Machol (*6*) observed the tellurium-rich phase boundary to be NiTe$_{1.9}$ (65.5 at % Te) at 712 °C. In an electron diffraction study on thin nickel telluride films Dvoryankina and Pinsker (*7*) found an alloy of the composition NiTe to be two-phase, and Kok, Wiegers and Jellinek (*8*) reported the nickel-rich phase boundary of the NiAs-phase to be NiTe$_{1.11}$ to NiTe$_{1.05}$ (52.7–51.3 at % Te) depending on temperature. Barstad, Grønvold, Røst, and Vestersjø (*9*) observed the range of homogenity of alloys annealed at 450 °C and slowly cooled to room temperature to be NiTe$_{1.09}$–NiTe$_{2.00}$ (52.2–66.6 at % Te).

From isopiestic measurements at 900 °C Shchukarev and Apurina (*5*) concluded the existence of three nickel-rich phases: NiTe$_{0.62}$ (38.3 at % Te), NiTe$_{0.66-0.67}$ to NiTe$_{0.82-0.83}$ (39.7–40.1 to 45.0–45.3 at % Te), and NiTe$_{0.88}$ (46.8 at % Te). Electron diffraction studies (*7*) revealed a phase of the approximate composition Ni$_3$Te$_2$ (40 at % Te) with two different structures. According to a preliminary

---

† All authors were formerly with New York University.

communication by Kok et al. (*8*), the NiAs-phase is in equilibrium with orthorhombic $NiTe_{0.9}$ (47.3 at % Te). In addition, they found a phase $Ni_{3\pm x}Te_2$ (± 40 at % Te) with a fairly broad range of homogeneity and a complex order-disorder transformation behavior with all structures related to the rickardite (Cu_3Te_2)-type crystal structure. At 700 °C nickel-rich $Ni_{3\pm x}Te_2$ (~ 37.5 at % Te) transformed reversibly to a tetragonal cell. In a careful phase analysis of nickel-rich alloys Barstad et al. (*9*) also described the existence of rickardite-related structures at $Ni_{3\pm x}Te_2$, with a range of homogeneity of 40.0–40.9 at % Te at 580 °C. Above 850° to 900 °C Ni_3Te_2 transformed to an f.c.c. structure. The lattice parameters of another orthorhombic phase, $NiTe_{0.77}$–$NiTe_{0.775}$ (43.5–43.6 at % Te) were found to agree with those of the $NiTe_{0.9}$ phase reported by Kok et al. (*8*). Stevels, Bouwma, and Weigers (*10*) studied the transformation behavior of $Ni_{3\pm x}Te_2$. At room temperature $Ni_{3+x}Te_2$ has an ordered monoclinic and $Ni_{3-x}Te_2$ an ordered tetragonal rickardite structure. With increasing temperature $Ni_{3\pm x}Te_2$ transformed to an ordered orthorhombic rickardite, a disordered tetragonal rickardite, an ordered f.c.c., and finally to a disordered f.c.c. structure.

From the heat of solution of NiTe in bromine water (*11*) an approximate heat of formation $\Delta H_f^0 = -9.67$ kcal/g-atom at 295 °K was calculated (*12*). Tilden (*13*) measured the mean heat capacity of NiTe, and Westrum, Chou, and Machol (*14*) determined the heat capacities of the δ phase at 52.3, 60.0, and 66.6 at % Te from 5 to 350 °K. Based on lattice energies derived from Kapustinskii's empirical equations Moody and Thomas (*15*) calculated the enthalpy of formation of NiTe. Westrum and Machol (*6*) measured dissociation pressures of Ni-Te alloys between 60 and 100 at % Te at temperatures up to 780 °C with a silica Bourdon gauge. Soboleva and Vasil'ev (*16*) determined the heat of formation of Ni-Te alloys between 50 and 60 at % Te at 900°–1000 °C and found them to be a linear function of composition.

It can be seen that the phase boundaries in the Ni-Te system are not well delineated and that thermodynamic information is quite incomplete. One objective of the study was to measure the thermodynamic activities of tellurium over the entire range of the NiAs-$Cd(OH)_2$ phase with an isopiestic method by equilibrating nickel specimens with tellurium vapor in a temperature gradient and to obtain the phase boundaries at various temperatures from the discontinuities in the specimen composition-temperature plots.

Experimental Procedures

Annular specimens 12-mm i.d. × 21-mm o.d. weighing about 50 mg were cut from a 1-mil 99.99% electrolytic nickel sheet (International Nickel Inc.). The blanks were cleaned in carbon tetrachloride, washed in reagent acetone and then weighed on a Mettler automatic analytic balance to an accuracy of ± 0.05 mg.

Graphite crucibles with press fit lids were machined from high-density (1.92 g/cm^3) graphite rods (Basic Carbon Corp.) that had a maximum ash content of less than 0.4%, and then baked out in vacuum (< 0.1 μ Hg) at 1000 °C for 2 h to remove any volatile material. The crucibles (Fig. *1*) were annular in shape 2.5-cm o.d. × 7-mm i.d. by 2-mm wall thickness and 1.5-cm over-all height, and had two 0.5-mm holes drilled through the sides. In some cases, grooves of approximately the same dimension (0.5 mm) were cut into the press fit lids. The grooves or holes allowed the tellurium vapor pressure to equalize inside and outside the crucibles during the equilibration, but were small enough to minimize tellurium losses during cooling.

After baking out the graphite, two of the preweighed nickel specimens were placed in each crucible, the lid put on and the crucibles containing the samples reweighed on the same balance. The crucibles weighed about 8 g each. The weighed carbon crucibles containing the nickel samples were then placed into a quartz tube 38-mm o.d. × 35-mm i.d. by 70 cm long that had an inner quartz thermocouple tube 3-mm i.d. by 5-mm o.d. × 45 cm long

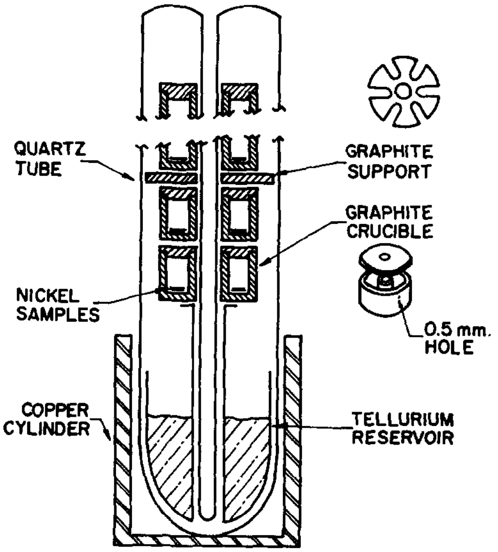

FIG. 1. Reaction assembly.

as shown in Fig. 1. The top of the quartz tube was attached to a standard taper joint to allow for evacuation. All quartz parts had been previously cleaned with hot cleaning solution and rinsed with distilled water, heated to 900 °C and back filled with argon before cooling. Thirty grams of 99.99% Asarco Inc. Te, melted and filtered under a vacuum of < 0.01 μ Hg and cast into a quartz crucible, served as the Te reservoir. It was loaded into the quartz tube, which was then evacuated to less than 0.01 μ Hg for 24 h and sealed under running vacuum.

After sealing, the sample positions were measured to an accuracy of ± 2 mm relative to the bottom of the inner thermocouple tube so that the temperature of the specimens and of the reservoir could be determined by lowering and raising a Pt-Pt 10% Rh thermocouple in the inner quartz thermocouple tube. The thermocouple was calibrated according to National Bureau of Standards procedure (*17*). In order to eliminate the effect of small temperature fluctuations on the temperature determination, the temperature was plotted versus distance along the reaction tube. A smooth curve was drawn through the slightly scattered points. Using this smooth curve and the previously determined specimen positions, an average sample temperature was determined.

The end of the quartz tube containing the tellurium reservoir was placed in a copper cylinder 4.5-cm i.d. × 6.5-cm o.d. × 10 cm high. This cylinder, which only reached to the first sample, created a constant temperature zone of ± 1 °C over the length of the reservoir. The quartz tube was tied with Nichrome V wire and lowered into a specially constructed vertical tube furnace with a gap of 7.5 cm between its upper and lower resistance windings. The upper and lower cores were separately controlled by an Esterline Angus controller and Pt-Pt 10% Rh thermocouple. This apparatus is capable of maintaining the temperature at any point constant to ± 2 °C during the duration of an experimental run. Temperature gradients from 250 °–400 °C along the furnace length were generated by varying the controller settings, with the temperature minimum at the reservoir being set at between 420 ° and 650 °C. The equilibration runs lasted from 1 to 3 weeks and were terminated by water quenching the quartz tubes. Very little evidence of tellurium evaporation from the samples and condensation on the quartz tube during quenching was observed. In subsequent runs, only every third sample was replaced by pure nickel sheet in order to achieve equilibration for adjacent samples from two directions. If the resulting composition of the specimens was a smooth function of activity, it would be a strong indication that the run had come to equilibrium.

The crucibles were again weighed after equilibration, and the difference in weight before and after equilibration was taken as the weight of tellurium absorbed. Since the specimens did not lose nickel during equilibration the only errors inherent in this method of analysis are the weighing errors. These combine to form an over-all error in the tellurium analysis of ± 0.1 at % Te.

Two possible extraneous errors could be introduced through the use of the graphite crucibles since graphite could react with tellurium and/or nickel during equilibration. These two errors were found to be negligible by two critical experiments. A graphite crucible was placed in an evacuated sealed quartz capsule with pure tellurium. The capsule was placed in a furnace at 800 °C such that the crucible was at a slightly higher temperature than the tellurium, to insure that the tellurium did not simply condense on the crucible. After nearly 3 weeks at temperature and subsequent slow cooling there was no detectable change in weight of the crucible. To check for possible reaction of graphite and nickel, a pure nickel-sheet sample was placed in a graphite crucible, sealed into an evacuated quartz capsule, and placed into a furnace at 950 °C for 2 weeks. The nickel was then removed and weighed; there was no detectable weight change of the nickel sample. It would seem that the over-all error in analysis of ± 0.1 at % Te is exclusively a weighing error which results in an average error in $\log a_{\mathrm{Te}}$ of ± 0.01 units. The uncertainty in determining the position of the samples introduces a comparable average error in $\log a_{\mathrm{Te}}$. Therefore, it can be concluded that the principal cause of the scatter of the data points is due to slight fluctuations from equilibrium. However, the mean of these points represents true equilibrium or else the points in Fig. 3 would not fall on straight lines.

Experimental Results

The experimentally determined specimen composition-temperature data and reservoir temperatures, T_R, for the various runs are given in Fig. 2. The phase boundaries at different temperatures have been delineated from the breaks in the experimental curves and are listed in Table I. For run 10 solid tellurium was used as reservoir and a very large temperature gradient was imposed on the specimen tube. The data points of this run do not

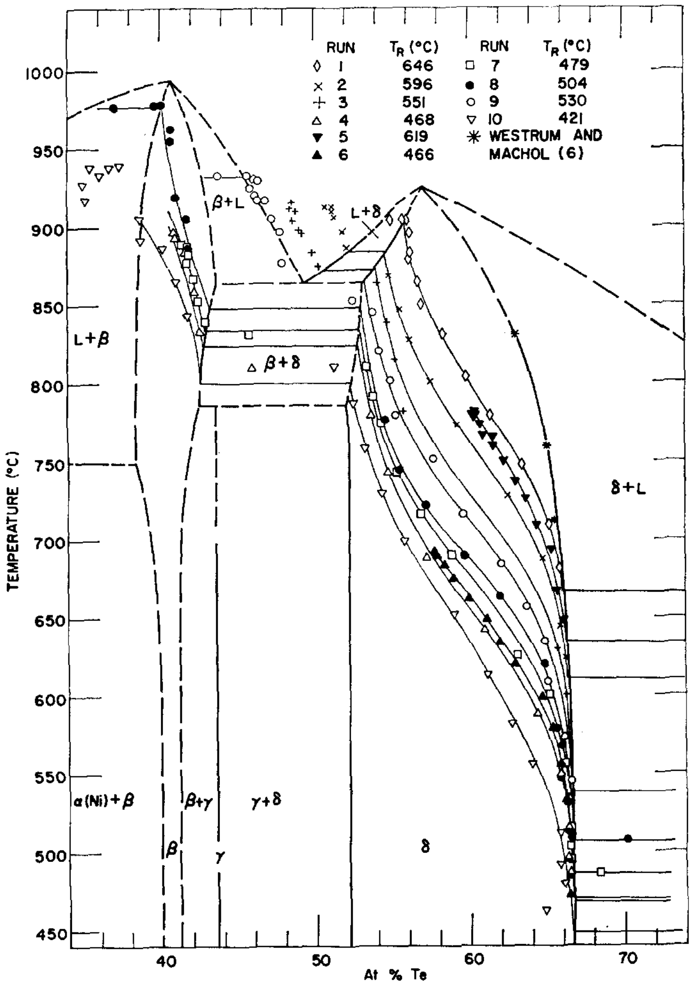

FIG. 2. Specimen composition versus specimen temperature partial Ni-Te phase diagram.

agree well with those of other runs and were not used in the computation of activities and partial molar enthalpies.

The activity of a component in an alloy can be expressed as the ratio of the vapor pressure of the component above the alloy divided by the vapor pressure of the pure component in the standard state at the temperature. Implicit in this definition is the assumption that the metal vapor contains only the monomer species. Although in the temperature range of our experiments tellurium in the vapor phase exists primarily as a dimer Te_2, the extent and the effect of dissociation has to be considered.

If dissociation is negligible, the activity of tellurium is expressed by

$$a_{Te} = (P_{Te_2})^{1/2}/(P_{Te_2})^{1/2}. \tag{1}$$

If dissociation of the vapor in equilibrium with the alloy is significant, then

$$a_{Te} = (P_{Te} + P_{Te_2}^{1/2})/(P_{Te_2}^{0})^{1/2}. \tag{2}$$

If dissociation of the vapor in equilibrium with the alloy and with the tellurium reservoir must be considered, then

$$a_{Te} = (P_{Te} + P_{Te_2}^{1/2})/(P_{Te}^{0} + P_{Te_2}^{0\,1/2}). \tag{3}$$

Budininkas, Edwards, and Wahlbeck (*18*) have determined the dissociation constant of Te_2 between 1067° and 1467°K. Dissociation will increase with increasing temperature and decreasing pressure. The effect on activities will, therefore, be most noticeable for alloys low in tellurium held at high temperatures. For the most extreme conditions in our experiments complete neglect of dissociation

TABLE I

PHASE BOUNDARIES IN THE Ni-Te SYSTEM

Comp. (at %Te)	Temp. (°C)	Run # or Ref.	Comp. (at %Te)	Temp. (°C)	Run # or Ref.
$(\delta + L)/L$ Boundary			$(L + \delta)/\delta$ Boundary		
99.75	448.7	(6)	53.3	866	#9
92.2	650	(6)	54.0	872	#3
90.0	682	(6)	54.6	884	#2
87.0	712.5	(6)	55.8	904	#1
82.0	760	(6)	$L/(L + \delta)$ Boundary		
$\delta/(\delta + L)$ Boundary			49.6	866	#9
66.6	448.7	(6)	50.5	872	#3
66.5	468	#6	52.2	884	#2
66.5	470	#4	$(\beta + L)/L$ Boundary		
66.5	486	#7	45.5	933	#9
66.6	507	#8			
66.6	538	#9	$\beta/(\beta + \delta)$ Boundary		
66.5	560	#3	42.6	800	#10
66.3	610	#2	42.8	824	#4
66.2	644	#5	43.0	834	#7
66.0	666	#1	43.2	848	#8
65.5	712.5	(6)	$(L + \beta)/\beta$ Boundary		
65.0	760	(6)	38.8	903	#10
63.0	830	(6)	40.1	977	#8
$(\beta + \delta)/\delta$ Boundary					
52.2	800	#10			
52.8	824	#4			
52.9	834	#7			
53.0	848	#8			

results in an error in the activities of less than 1%. Therefore, Eq. (1) was employed to compute all activity values.

In the experiments tellurium was transferred from the reservoir into the nickel samples which were kept in a constant temperature gradient until at equilibrium the vapor pressure of tellurium over each of these samples was the same as that of the pure tellurium reservoir maintained at the temperature minimum. The activity is then the square root of the vapor pressure of pure tellurium at the reservoir temperature divided by the vapor pressure of pure tellurium at the sample temperature,

$$a_{\mathrm{Te}} = \left(\frac{P^0_{\mathrm{Te}_2}\ \text{Reservoir Temp.}}{P^0_{\mathrm{Te}_2}\ \text{Sample Temp.}} \right)^{1/2}. \tag{4}$$

The standard states chosen for this study are pure liquid tellurium and solid nickel. The vapor pressure of tellurium was taken from Brebrick (*19*) which agreed well with previous investigations.

Partial molar enthalpies have been computed from the activity data using a form of the Clausius-Clapeyron equation derived by Birchenall and Cheng (*20*):

$$\frac{1}{T_R} = \frac{\Delta H}{\Delta H^0_V} \frac{1}{T_S} + C. \tag{5}$$

T_S is the specimen temperature, C an integration constant, ΔH^0_V the enthalpy of vaporization of pure tellurium and ΔH the enthalpy change corresponding to the transfer of tellurium from a sample to the vapor phase. ΔH is computed as follows:

$$\begin{array}{lll} 2\mathrm{Te}_{(L)} \rightarrow \mathrm{Te}_{2(g)} & \Delta H^0_V & \\ 2\mathrm{Te}_{(\mathrm{alloy})} \rightarrow 2\mathrm{Te}_{(L)} & -2\Delta \bar{H}_{\mathrm{Te}} & \\ \hline 2\mathrm{Te}_{(\mathrm{alloy})} \rightarrow \mathrm{Te}_{2(g)} & \Delta H = \Delta H^0_V - 2\Delta \bar{H}_{\mathrm{Te}}. & (6) \end{array}$$

From Fig. 2 sample temperatures were interpolated at fixed compositions and the interpolated reciprocal sample temperatures were plotted as a function of the reciprocal reservoir temperatures in Fig. 3. From the slopes of these straight lines the partial molar enthalpies of tellurium of the samples

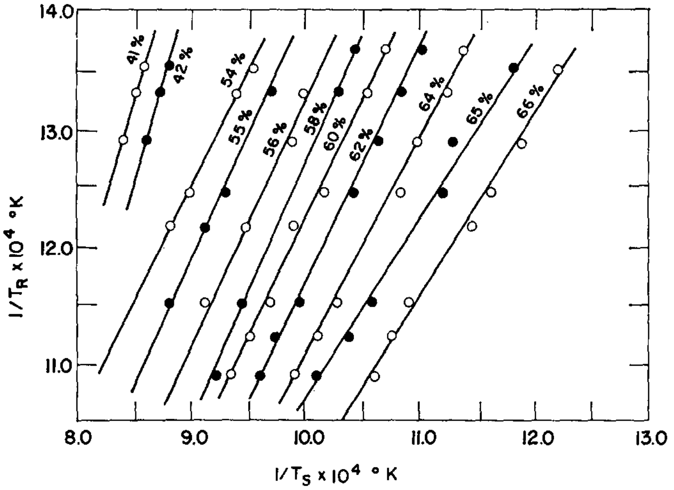

FIG. 3. Reciprocal reservoir temperature versus reciprocal sample temperature.

were calculated by Eqs. (5) and (6). The value of ΔH_V^0 of 27.4 kcal/g-mole of Te_2 was taken from Brebrick (*19*). The calculated partial molar enthalpies of tellurium are listed in Table II and are plotted as a function of composition in Fig. 4.

Inserting the partial molar enthalpies into the Gibbs-Helmholtz equation the activities were corrected to a single common temperature. The corrected activities at 600° and 875 °C are shown in Fig. 5. Partial molar-free energies and entropies were computed and are also given in Table II and plotted in Fig. 4.

Discussion

The phase boundary data in Fig. 2 and Table I confirm a very wide solubility range for the NiAs-$Cd(OH)_2$ δ phase. The stoichiometric composition $NiTe_2$ is reached, but not exceeded. The tellurium-rich boundary occurs at 66.6 at % Te at low temperatures, and shifts increasingly rapidly toward lower tellurium concentrations with increasing temperature. There is excellent agreement between the phase limits determined by Westrum and Machol (*6*) and the present work. The limiting composition at 900 °C of 63 at % Te as determined by Shchukarev and Apurina (*5*) seems to be in the liquid region and is, therefore, incorrect. For the nickel-rich boundary of the δ phase the data of Kok et al. (*8*) and Barstad et al. (*9*) are confirmed which indicate the stoichiometric NiTe is not stable and that the compound does not exist beyond 52 at % Te on the nickel-rich side.

At elevated temperatures the β phase exists over a fairly wide range of homogeneity. The solubility limits at 900 °C were determined to be approximately 39–43 at % Te which is in reasonable agreement with the value of Shchukarev and Apurina (*5*) of 40–45 at % Te. Our data are not sufficient to verify any of the solid-solid transformations reported by other authors in the β phase and to determine whether the compound at 36 at % Te exists, as reported by Kok et al. (*8*) and Shchukarev and Apurina (*5*). However, the fact that the data points in Fig. 2 appear to be essentially temperature independent in this region suggests that this compound, if present, has a noncongruent melting point.

Since we found no indication of a compound between β and δ above 800 °C, the γ phase, reported by Barstad et al. (*9*) and Kok et al. (*8*), most probably decomposes by a peritectoid reaction to β and δ at some temperatures below 800 °C. The phase diagram in Fig. 2 is drawn accordingly. Shchukarev and Apurina (*5*) reported the compound $NiTe_{0.88}$ to be stable at 900 °C. According to our data, alloys in this temperature range are liquid and this compound was probably formed during solidification, and may be identical with the γ phase. The liquidus is outlined by our data points of runs 1, 2, 3, and 9, and the eutectic point between the congruent melting compounds β and δ is tentatively given at 49 at % Te and 865 °C.

The activity data at 600° and 875 °C are shown in Fig. 5. At 66.6 at % Te the slope of the activity curve is almost vertical and decreases with decreasing Te content. At about 59 at % Te the curve has an inflection point and then the slope begins to increase with decreasing Te content. The three data points obtained by Westrum and Machol (*6*) between

TABLE II

PARTIAL MOLAR THERMODYNAMIC QUANTITIES OF SOLID Ni-Te ALLOYS

Comp. (at % Te)	$-\Delta H_{Te}$ (kcal/g-atom)	$-\Delta S_{Te}$ (e.u.)	$-\Delta\bar{G}_{Te}$ (875°C) (kcal/g-atom)	$-\log a_{Te}$ (875°C)	$-\Delta\bar{G}_{Te}$ (600°C) (kcal/g-atom)	$-\log a_{Te}$ (600°C)	$-\log a_{Te}$ (600°C) (calc.)
66.6	7.0	7.9	—	—	0.12	0.03	∞
66.0	7.6	7.3	—	—	1.23	0.31	0.48
65.0	8.5	7.5	—	—	1.97	0.50	0.72
64.0	11.9	11.1	—	—	2.62	0.66	0.85
63.0	13.5	11.7	—	—	3.27	0.81	0.94
62.0	14.0	11.9	—	—	3.65	0.92	1.03
61.0	14.5	11.8	—	—	4.20	1.06	1.10
60.0	15.1	12.2	1.20	0.24	4.48	1.13	1.17
59.0	14.9	11.6	1.60	0.31	4.74	1.20	1.25
58.0	14.9	11.0	2.20	0.42	5.27	1.32	1.32
57.0	14.9	10.6	2.64	0.51	5.60	1.41	1.40
56.0	14.7	10.0	3.26	0.63	5.95	1.50	1.49
55.0	14.9	9.7	4.05	0.78	6.45	1.63	1.58
54.0	14.6	8.6	4.83	0.93	7.10	1.79	1.70
53.0	14.9	8.2	—	—	7.73	1.95	1.83
42.0	35.0	25.2	6.06	1.17	—	—	—
41.0	38.0	26.0	8.15	1.58	—	—	—
40.0	41.0	26.4	10.70	2.07	—	—	—

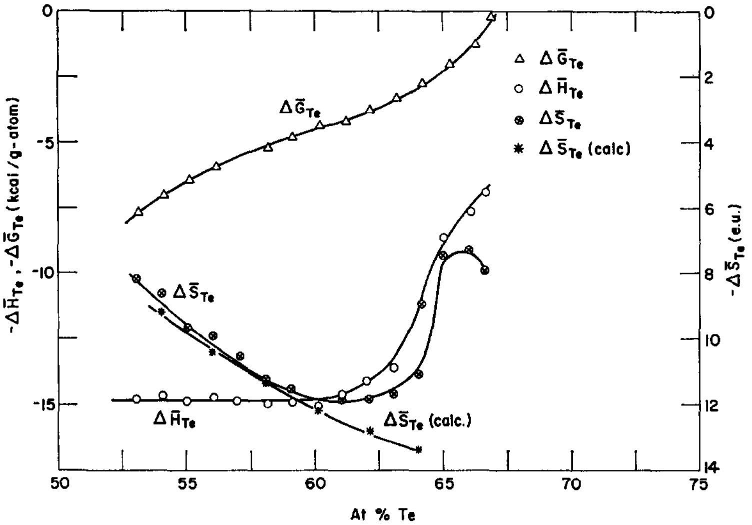

FIG. 4. Partial molar thermodynamic quantities of Ni-Te alloys.

66.6 and 63 at % Te agree well with our data. The activity curve at 875 °C shows the three single phase regions which exist at this temperature: δ, L, and β.

The partial molar thermodynamic properties are plotted in Fig. 4. The significant characteristic of the partial molar enthalpy-composition curve is the composition independence of $\Delta\bar{H}_{Te}$ in the single phase region between 52 and 60 at % Te. The absolute $\Delta\bar{H}_{Te}$ values then decrease with increasing Te content. Hultgren et al. (*12*) have calculated $\Delta\bar{H}_{Te}$ from the data reported by Westrum and Machol (*6*) and the values are also shown in Fig. 4. At 60 and 62 at % Te excellent agreement is obtained with our value of −14.8 kcal/g-atom. Soboleva and Vasil'ev (*16*) found that the enthalpy of formation of Ni-Te alloys between 900° and 1000 °C increases linearly from −6.4 kcal/g-atom at 50 at % Te to −6.9 kcal/g-atom at 60 at % Te. From these data,

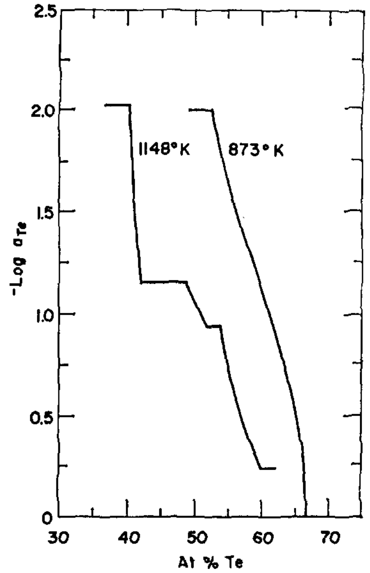

FIG. 5. Tellurium activities in the Ni-Te system at 600° and 875°C.

a constant $\Delta \bar{H}_{Te}$ of −8.6 kcal/g-atom is obtained. According to the phase diagram in Fig. 2, the alloys investigated by Soboleva and Vasil'ev were predominantly liquid. The heat of formation of solid alloys must be more negative than the heat of formation of liquid alloys by the heat of fusion of the alloy. It is also expected that the heat of fusion of the alloy would tend to increase with increasing Te content owing to the higher heat of fusion of Te. This correction would bring the data of Soboleva and Vasil'ev more in line with ours.

In $NiTe_2$ the tellurium atoms have essentially a hexagonal close packed arrangement, with the Ni atoms occupying every other layer of the octahedral sites. Increasing the Ni content from $NiTe_2$ towards NiTe takes place by inserting Ni atoms in the 00 1/2 layers as shown in Fig. 6. At the ideal stoichiometric composition NiTe, all layers of Ni atoms should be completely filled. According to the measurements of Barstad et al. (9), the lattice parameters a and c, and the c/a ratio increase initially with increasing Ni content starting from $NiTe_2$. The a lattice parameter continues to increase over the entire δ phase composition region, while the c parameter passes through a flat maximum at 54 at % Te. The c/a ratio shows a distinct maximum at 61 at % Te. At about the same composition, a sharp break occurs in the $\Delta \bar{H}_{Te}$ versus composition curve as shown in Fig. 4. The $\Delta \bar{H}_{Te}$ data indicate that in the composition region from 52–60 at % Te, the energy required to add a nickel atom to the compound is independent of composition. From 60–66 at % Te the enthalpy change on addition of a nickel atom to the compound decreases sharply with composition. These breaks correspond closely to the composition at which 25% of the sites in the 00 1/2 layers are occupied by Ni atoms. At 25% occupancy, an ordered arrangement of Ni atoms in the 00 1/2 layers permits a Ni atom to have no other atoms as nearest neighbors in the layer.

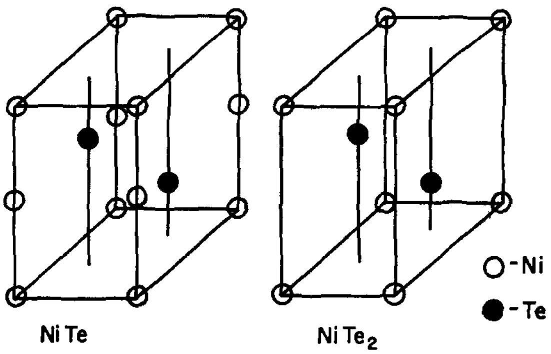

FIG. 6. Unit cells of NiTe and $NiTe_2$.

The published X-ray data obtained by the Debye-Scherrer method would not be expected to show evidence of such order. The $\Delta \bar{H}_{Te}$ data could therefore be interpreted as indicating that below 25% occupancy of nickel sites in the 00 1/2 layers the nickel atoms occupy preferentially ordered positions. Above 25% occupancy additional nickel atoms are introduced randomly resulting in composition independent $\Delta \bar{H}_{Te}$ values.

In the region from 52–60 at % Te, a statistical model assuming random distribution of nickel atoms in the 00 1/2 layers should be satisfactory. The grand partition function of such a compound is

$$(\text{G.P.F.}) = Q_0 \sum \frac{M_{00\,1/2}!}{M_v!(M_{00\,1/2} - M_v)!} \times \lambda_{Ni}^{-M_v} K^{-M_v} \exp\left[\frac{-M_v E_v}{kT}\right]. \quad (7)$$

Q_0 is the grand partition function of the ideal stoichiometric compound NiTe, $M_{00\,1/2}$ and M_v are the total number of sites in the 001/2 layers and the number of unoccupied sites in these layers, respectively, λ_{Ni} is the absolute activity of nickel, K is the term for non-configurational contributions, and E_v is the energy of formation of a vacancy in the 00 1/2 layer. The relationship between the number of vacancies and the deviation from the stoichiometric composition $\Delta N_{Te}^* = N_{Te} - 0.5$ is

$$\Delta N_{Te}^* = M_v/2(M_s - M_v), \quad (8)$$

where M_s is the total number of sites and $M_{00\,1/2}$ is,

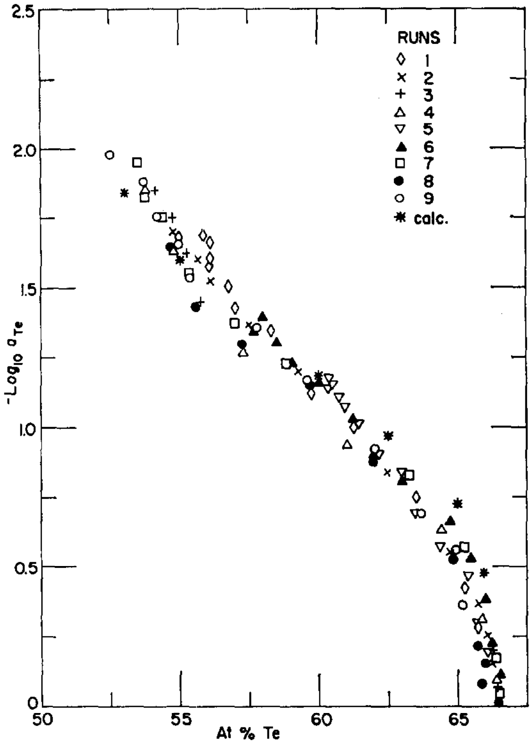

FIG. 7. Experimental and theoretical tellurium activities of Ni-Te alloys at 600°C.

therefore, equal to $M_s/4$. Solving the (G.P.F.) by the maximum term method we obtain

$$\ln \lambda_{Ni} = \ln\left(\frac{1 - 6\Delta N^*_{\mathrm{Te}}}{8\Delta N^*_{\mathrm{Te}}}\right) - \ln K - \frac{E_v}{kT}. \quad (9)$$

The activity of tellurium was calculated by a Gibbs-Duhem integration:

$$\ln \lambda_{\mathrm{Te}} = \ln\left\{\frac{(N_{\mathrm{Te}} - 0.5)}{[N_{\mathrm{Te}}(0.666 - N_{\mathrm{Te}})]^{1/2}}\right\} + \text{const.} \quad (10)$$

This equation shows an inflection point at 58.3 at % Te in excellent agreement with the inflection point of the experimental activity curve. Activity values were calculated from Eq. (10), choosing the constant so that the calculated value matched the experimental value at the inflection point. The calculated and experimental activities at 600°C are given in Table II and Fig. 7. The calculated values agree quite closely with the experimental points in the region of constant $\Delta\bar{H}_{\mathrm{Te}}$ (52–60 at % Te) as expected. At higher tellurium concentrations where $\Delta\bar{H}_{\mathrm{Te}}$ varies with composition the calculated activities show increasing deviations. Anderson (*21*) has suggested that in nonstoichiometric compounds interactions between defects may be significant. If such interactions occur, then an additional vacancy interaction term, $\exp[-(z/2)(M_v/M_{00\,1/2})^2(E_i/kT)]$, should be included in the (G.P.F.), where $z = 6$, the number of nearest neighbors of a nickel atom in the 00 1/2 layer and E_i, the interaction energy between nickel vacancies. This introduces an additional term $-(12E_i/M_{00\,1/2}kT)(\Delta N^*_{\mathrm{Te}}/(1 + 2\Delta N^*_{\mathrm{Te}}))$ in Eq. (9) and a term $+(6E_i/M_{00\,1/2}kT)[\frac{1}{3}\ln N_{\mathrm{Te}} - (2N^2_{\mathrm{Te}} - 1)/2N_{\mathrm{Te}}]$ in Eq. (10). Regardless of the value of E_i chosen the fit between calculated and experimental points could not be improved. The best agreement was obtained when no interaction was assumed. For a random arrangement of nickel atoms in the 00 1/2 layers, partial molar entropies of tellurium were calculated from Eq. (10) according to

$$\Delta\bar{S}_{\mathrm{Te}} = (\Delta\bar{H}_{\mathrm{Te}}/T) - R\ln\lambda_{\mathrm{Te}}$$

$$= -R\ln\frac{(N_{\mathrm{Te}} - 0.5)}{[N_{\mathrm{Te}}(0.666 - N_{\mathrm{Te}})]^{1/2}} + \text{const.} \quad (11)$$

The constant was chosen by arbitrarily matching the calculated value with the experimental value at 58 at % Te. The calculated values are also plotted in Fig. 4. The excellent agreement between calculated and experimental partial molar entropies and activities in the region from 53–60 at % Te, where $\Delta\bar{H}_{\mathrm{Te}}$ is constant, strongly supports the concept that the nickel atoms occupying the 00 1/2 planes in the δ NiAs-Cd(OH)$_2$ compound are randomly arranged. The deviation between experimental and calculated values at higher tellurium concentrations could not be explained by assuming nearest neighbor interaction between the nickel vacancies, and, therefore the possibility exists that the deviation in this composition range is caused by long-range order.

Acknowledgment

The work was supported by the Atomic Energy Commission under the Contract AT(30-1)-3955. The authors gratefully acknowledge the support and interest of Dr. L. Ianiello of the Atomic Energy Commission.

References

1. I. OFTEDAL, *Z. Phys. Chem.* **128**, 135 (1927).
2. S. TENGÉR, *Z. Anorg. Allgem. Chem.* **239**, 126 (1938).
3. W. KLEMM AND N. FRATINI, *Z. Anorg. Allgem. Chem.* **251**, 222 (1943).
4. A. SCHNEIDER AND K. H. IMHAGEN, *Naturwissenschaften* **44**, 324 (1957).
5. S. A. SHCHUKAREV AND M. S. APURINA, *Russ. J. Inorg. Chem.* **5**, 1167 (1960).
6. E. F. WESTRUM AND R. F. MACHOL, *J. Chem. Phys.* **29**, 824 (1958).
7. G. DVORYANKINA AND Z. PINSKER, *Kristallografiya* **7**, 458 (1962); English transl., *Soviet Phys. Cryst.* **8**, 448 (1964).
8. R. G. KOK, G. A. WIEGERS, AND F. JELLINEK, *Rec. Trav. Chim. Pays. Bas.* **84**, 1585 (1965).

9. J. Barstad, F. Grønvold, E. Røst, and E. Vestersjø, *Acta Chem. Scand.* **20**, 2865 (1966).
10. A. L. N. Stevels, J. Bouwma, and G. A. Wiegers, *2nd Intern. Conf. Solid Comp. Trans. Elements*, Twente (1967).
11. C. Fabre, *Compt. Rend.* **105**, 277 (1887).
12. R. Hultgren, R. L. Orr, P. D. Anderson, and K. K. Kelley, "Selected Values of Thermodynamic Properties of Metals and Alloys," John Wiley and Sons, Inc., New York, 1963.
13. W. A. Tilden, *Trans. Roy. Soc.* **A203**, 139 (1904).
14. E. F. Westrum, C. Chou, R. E. Machol, and F. Grønvold, *J. Chem. Phys.* **28**, 497 (1958).
15. G. Moody and J. Thomas, *J. Chem. Soc. London* 1417 (1964).
16. M. S. Soboleva and Ya. Vasil'ev, *Vestn. Leningrad Univ. Ser. Fiz. Khim.* **3**, 153 (1962); *C.A.* **58**, 981f (1968).
17. W. F. Roeser and S. Lonberger, *Natl. Bur. Std.* (U.S.), Circ. No. 590 (1956).
18. P. Budininkas, R. K. Edwards, and P. G. Wahlbeck, *J. Chem. Phys.* **48**, 2870 (1968).
19. R. F. Brebrick, *J. Phys. Chem.* **72**, 1032 (1968).
20. C. E. Birchenall and C. H. Cheng, *Trans. Met. Soc. AIME* **185**, 438 (1949).
21. J. S. Anderson: *Proc. Roy. Soc. London* **A185**, 69 (1946).